Signal propagation parameters estimation through designed multi layer fibre with higher dominant modes using OptiFibre simulation

Article *in* Journal of Optical Communications · June 2022

DOI: 10.1515/joc-2021-0213

12 authors, including:

Ahmed Nabih Zaki Rashed
faculty of electronic engineering menoufia university

Hasane Ahammad Shaik
K L University

Malek G. Daher
Islamic University of Gaza

Vishal Sorathiya
Parul Universiy

Ahmed Nabih Zaki Rashed*, SK. Hasane Ahammad, Malek G. Daher, Vishal Sorathiya, Abrar Siddique, Sayed Asaduzzaman, Hasin Rehana, Nitul Dutta, Shobhit K. Patel, Vincent Omollo Nyangaresi, Rayhan Habib Jibon and Anas Ibrahim

Signal propagation parameters estimation through designed multi layer fibre with higher dominant modes using OptiFibre simulation

https://doi.org/10.1515/joc-2021-0213
Received September 11, 2021; accepted May 30, 2022; published online June 23, 2022

Abstract: The aim and scope of the paper is to simulate the signal propagation parameters estimation through designed multi-layer fibre with higher dominant modes by using OptiFibre simulation software. The multi-layer fibre profile has a length of 1000 m is designed and clarified with six layers. RI difference profile variations are clarified with radial distance variations. Modal/group index, group delay, dispersion, mode field diameter and total fibre losses are demonstrated with the fibre wavelength variations. All the dominant mode field distribution for multi-layer fibre are simulated and demonstrated. The other modes for designed multi-layer fibre with the theoretical fibre cutoff values for the different modes based the designed multi-layer fibre are analyzed and clarified clearly in details.

Keywords: dominant modes; multi layer fibre; parameters estimation; signal propagation.

***Corresponding author: Ahmed Nabih Zaki Rashed**, Electronics and Electrical Communications Engineering Department, Faculty of Electronic Engineering, Menoufia University, Menouf, 32951, Egypt, E-mail: ahmed_733@yahoo.com. https://orcid.org/0000-0002-5338-1623
SK. Hasane Ahammad, Department of ECE, Koneru Lakshmaiah Education Foundation, Vaddeswaram, Andhra Pradesh, 522302, India, E-mail: ahammadklu@gmail.com
Malek G. Daher, Physics Department, Islamic University of Gaza, P.O. Box 108, Gaza, Palestine, E-mail: malekjbreel20132017@gmail.com
Vishal Sorathiya, Department of Information and Communication Technology, Marwadi University, Rajkot, India, E-mail: vishal.sorathiya9@gmail.com
Abrar Siddique, Department of Smart Robot Convergence and Application Engineering, Pukyong National University, Busan, 48513, Korea; and Department of Electrical and Computer Engineering, University of Waterloo, Waterloo, ON N2L 3G1, Canada, E-mail: abrarkhokhar.iiui@gmail.com
Sayed Asaduzzaman and Hasin Rehana, Department of Computer Science and Engineering, Rangamati Science and Technology University, Rangamati, Bangladesh; and Department of Computer Science and Engineering, Daffodil International University, Dhaka, Bangladesh, E-mail: asadcse.rmstu@gmail.com (S. Asaduzzaman), hasin.cse13@gmail.com (H. Rehana). https://orcid.org/0000-0002-8556-3691 (S. Asaduzzaman)
Nitul Dutta, Computer Science and Engineering Department, SRM University, Guntur, Andhra Pradesh, India, E-mail: nituldutta@gmail.com
Shobhit K. Patel, Computer Science and Engineering Department, SRM University, Guntur, Andhra Pradesh, India; and Electronics and Communication Engineering Department, Marwadi University, Rajkot, Gujarat, India, E-mail: shobhitkumar.patel@marwadieducation.edu.in
Vincent Omollo Nyangaresi, Tom Mboya University College, P.O. Box 199-40300, Homabay, Kenya, E-mail: vnyangaresi@tmuc.ac.ke
Rayhan Habib Jibon, Electronics and Communication Engineering Discipline, Khulna University, Khulna, 9208, Bangladesh, E-mail: jibon.ece.ku@gmail.com
Anas Ibrahim, Electronics and Electrical Communications Engineering Department, Faculty of Electronic Engineering, Menoufia University, Menouf, 32951, Egypt, E-mail: anasibrahim453@yahoo.com

1 Introduction

Imperfection losses include bending, coupling and splicing losses [1–9]. They arise because of stress from the manufacturing, environment and physical bending. Joint or splicing losses arise from inherent problems of connection when jointing fibres like different diameters of core and/or cladding, different relative index differences and/or numerical aperture, different RI profiles and fibre faults [10–18]. The configurations of optical fibres can be further categorized according to both of the index profile of fibre and the modes propagating through it into three types. The SMF-SI fibre has a central core which is significantly small such that there is only one light path for propagation within fibre. The core diameter of SMF-SI fibre is smaller (8–12 μm) than that of MMFs. In the SMF-SI, all light rays arrive at the same time to the end. Manufacturing and handling of SMF-SI fibre is so difficult [12]. The MMF-SI fibre is the simplest type. It includes glass, PCS and plastic fibres. Its fabrication is easy. It has a core diameter (50–1000 μm) [19–28].

This leads to large aperture enabling more light to enter the fibre. Light rays travel in a zigzag path. There are many pathways that light ray takes during propagation [29–36]. MMF-SI fibre has profile index that takes steps from low to high and from high to low when measuring from cladding to core to cladding. The drawback of MMF-SI fibre is the different lengths of optical paths caused by various angles of light propagation [37–44].

The good results can be achieved with the same or compatible fibres. But there are still some jointing problems like mechanical alignment between two fibres being to be jointed, the quality of end-face of fibre and cleanliness of end-faces of fibre. The possible misalignment may result in three dimensions which are [45–54]: the longitudinal misalignment (the separation between fibres). The effective acceptance angle of the graded index (GI) fibre is slightly less than step index (SI) fibre. This makes coupling fibre to the light source more difficult. GI fibre has a higher bandwidth and a lower coupling efficiency than the SI fibre [55–61]. It is commercially available in sizes of 50/125 and 62.5/125. The 50/125 fibre with a smaller NA and higher bandwidth is improved for long haul communications [62–78]. The 62.5/125 fibre is enhanced for LAN networks [79–98].

2 Multi-layer fibre profile description

Figure 1 demonstrates the multi-layer fibre profile description. The fibre construction composed of six layers. Region 0 (first fibre layer) has a constant refractive index (RI) profile of 1.45 with 10 µm width. Region 1 (second fibre layer) has a parabolic fibre profile with the starting RI of 1.445 and ending RI of 1.4456 with 10 µm width. Region 2 (third fibre layer) has exponential RI profile with the starting RI of 1.445 and ending RI of 1.45 with width of 20 µm. The fibre wavelength varies from 0.85 to 1.65 µm. The designed multilayer fibre has 1000 m length of and 20 m coupling length.

Region 3 (fourth fibre layer) has a Gaussian fibre profile with max RI of 1.445, normalized full width half max (FWHM) value of 10 with 30 µm width. Region 4 (fifth fibre layer) has alpha peak fibre profile with max RI of 1.445, normalized index difference (NID) value of 0.4 and alpha value of 2 with 10 µm width. Region 5 (sixth fibre layer) has alpha dip fibre profile with max RI of 1.445, NID value of 0.4 and alpha value of 2 with 10 µm width. The designed multilayer fibre model description is clarified against radial distance (x) in Figure 1. The six fibre layers are composed of the alpha–dip, linear, parabolic, exponential, Gaussian and alpha–peak fibre profiles which are estimated by [10, 11, 19–22]:

$$n(x) = n_{\max} \exp\left[-\ln 2.\left(\frac{2(x - x_0)}{h.w}\right)\right]^2 \text{[Gaussian Profile]} \quad (1)$$

$$n(x) = n_{\max} \sqrt{1 - 2\Delta\left(\frac{x}{w}\right)^{\alpha}} \text{[Alpha Peak Profile]} \quad (2)$$

$$n(x) = n_{\max} \sqrt{1 - 2\Delta\left(1 - \frac{x}{w}\right)^{\alpha}} \text{[Alpha dip Profile]} \quad (3)$$

$$n(x) = n(0) + x.\frac{n(w) - n(0)}{w} \text{[Linear Profile]} \quad (4)$$

$$n(x) = [n(w) - n(0)].\left(\frac{x}{w}\right)^2 + n(0) \text{[Parabolic Profile]} \quad (5)$$

$$n(x) = [n(w) - n(0)].\frac{e}{e-1}\exp\left(-\frac{x}{w}\right) + \frac{e.n(w) - n(0)}{e-1} \text{[Exponential Profile]} \quad (6)$$

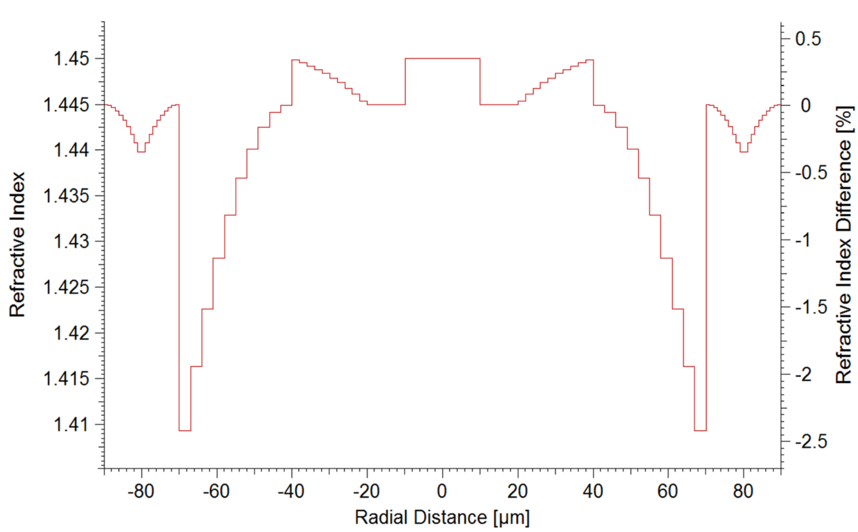

Figure 1: Designed multi-layer fibre model description.

with x is the radial distance, w is the layer width, $n_{\max}$ is the max value, x_0 is the position and Δ is the difference is represented by the following formula [10, 11, 19]:

$$\Delta = \frac{n_{\max}^2 - n_{\min}^2}{2 n_{\max}^2} \tag{7}$$

The group delay, total dispersion and the effective mode field diameter can represented by the following formulas [7, 19–22]:

$$T_g = -\frac{2\pi c z}{\omega^2}\left(k_0\frac{dn}{d\lambda} + n\frac{dk_0}{d\lambda}\right) = \frac{z}{c}\left(n - \lambda\frac{dn}{d\lambda}\right) \tag{8}$$

$$D_{\text{total}} = -\frac{z\lambda}{c}\left(\frac{d^2 N_{\text{eff}}}{d\lambda^2}\right) \tag{9}$$

$$d_{\text{eff}} = \frac{2}{\sqrt{\pi}}\sqrt{A_{\text{eff}}} \tag{10}$$

with the wave number $k_0 = 2\pi/\lambda$, A_{eff} is the effective area. Where the macro and micro-fibre losses are estimated by [6, 19–21]:

$$\alpha_{\text{macro}} = \frac{10}{z}\log(\exp[\gamma z]) \tag{11}$$

$$\alpha_{\text{micro}} = A(kn_1 d_n)^2 (kn_1 d_n^2)^{2p} \tag{12}$$

with A is a constant, p is the exponent power law. The splice losses can be given by [6, 7, 10, 11, 19–22]:

$$\alpha_{\text{Splice}} = -10\log\left[\left(\frac{16 n_1^2 n_2^2}{(n_1+n_2)^4}\right)\frac{\sigma}{q}\exp\left(\frac{-\rho u}{q}\right)\right] \tag{13}$$

where the parameters ρ, q are calculated by the following formulas [7, 10, 19–21]:

$$\rho = \frac{(k w_1^2)}{2} \tag{14}$$

$$q = G^2 + \frac{(\sigma+1)^2}{4} \tag{15}$$

with the parameters σ and G are estimated by [6, 7, 11, 19–21]:

$$\sigma = \left(\frac{w_2}{w_1}\right)^2 \tag{16}$$

$$G = \frac{z}{k\ w_1^2} \tag{17}$$

3 Results and discussions

We have simulated the designed multi-layer fibre by using optifibre simulation software. The model/group RI are analyzed and sketched with fibre wavelength variations. All the fibre losses and fibre dispersion are simulated and clarified in more details. All the fibre linear polarization (LP) modes and the theoretical fibre cutoff values for the different modes based the designed fibre profile model are detected and clarified by using the finite difference method.

Figure 2 demonstrates the group/model indices variations with the variations of the fibre wavelength. The modal index decreases exponentially through the fibre wavelength of 0.85–1.2 μm and increases exponentially through the fibre wavelength of 1.21–1.65 μm. But the group index decreases linearly through the fibre wavelength of 0.85–1.65 μm. Figure 3 shows the group delay variations in

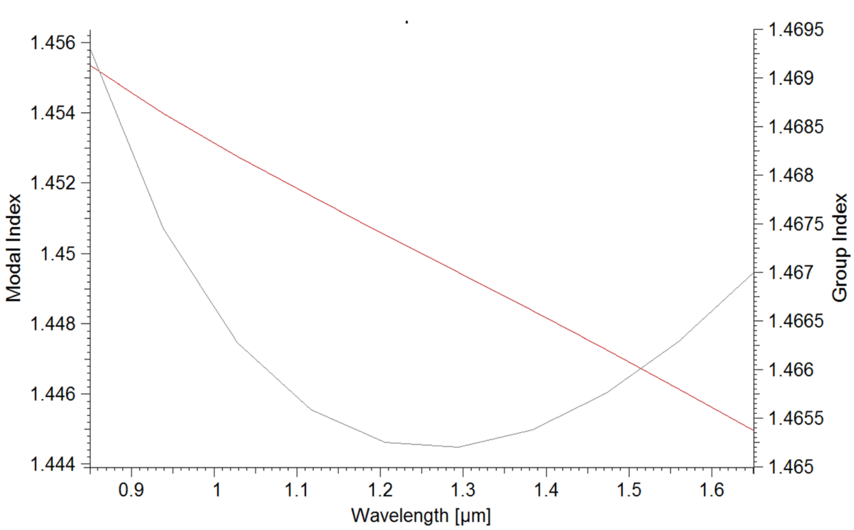

Figure 2: Group/model indices variations with the variations of the fibre wavelength.

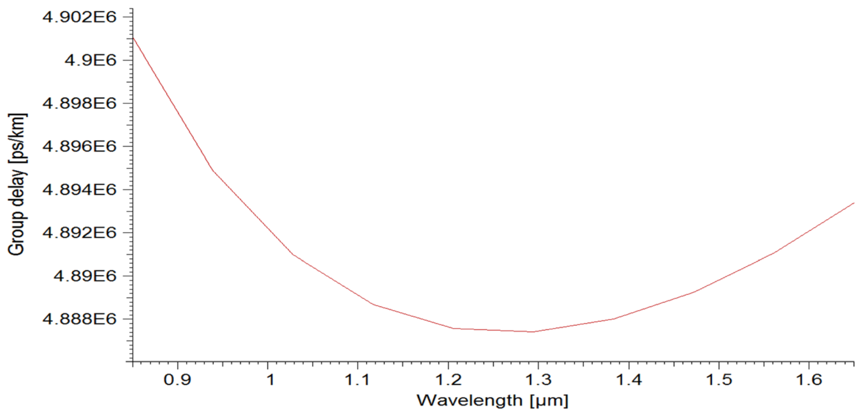

Figure 3: Group delay variations in relation to the fibre wavelength variations.

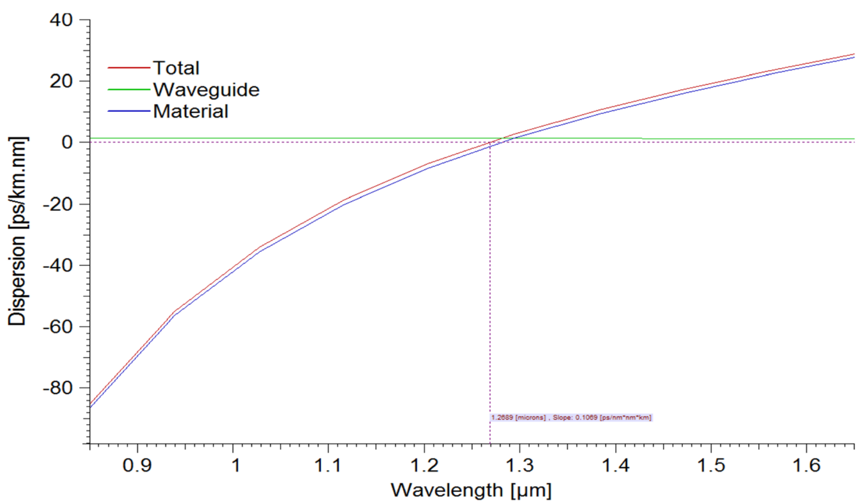

Figure 4: The fibre dispersion variations with respect to wavelength.

relation to the fibre wavelength variations. The group delay decreases exponentially through the fibre wavelength of 0.85–1.25 μm and increases exponentially through the fibre wavelength of 1.25–1.65 μm. The min fibre group delay is achieved at 1.25 μm which its value is 4.882 μs/km.

Figure 4 indicates the fibre dispersion variations with fibre wavelength variations. The dispersion is slightly constant at a value of 1 ps/nm.km. The fibre material dispersion increases exponentially with the fibre wavelength variations. Therefore the resultant total fibre dispersion increases exponentially with the fibre wavelength. The zero dispersion for the designed multi-fibre layers is at 1.2689 μm and the slope of dispersion is 0.1069 ps/nm^2 km for the designed fibre.

Figure 5 shows the mode field diameter/effective area variations with wavelength. The far and near fibre field

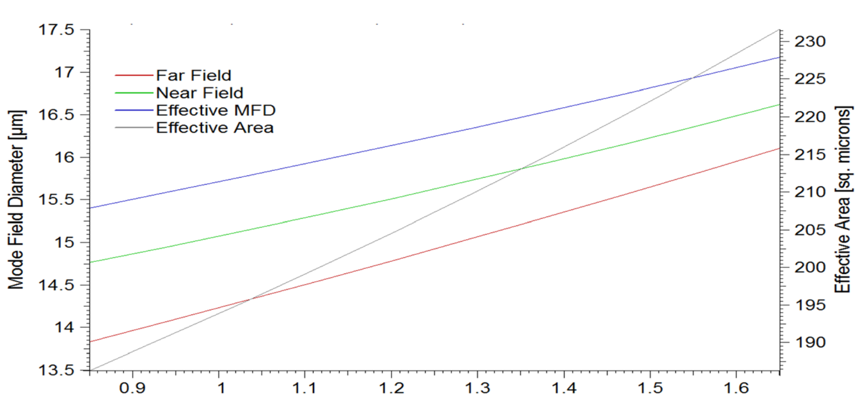

Figure 5: The mode field diameter/effective area variations with wavelength.

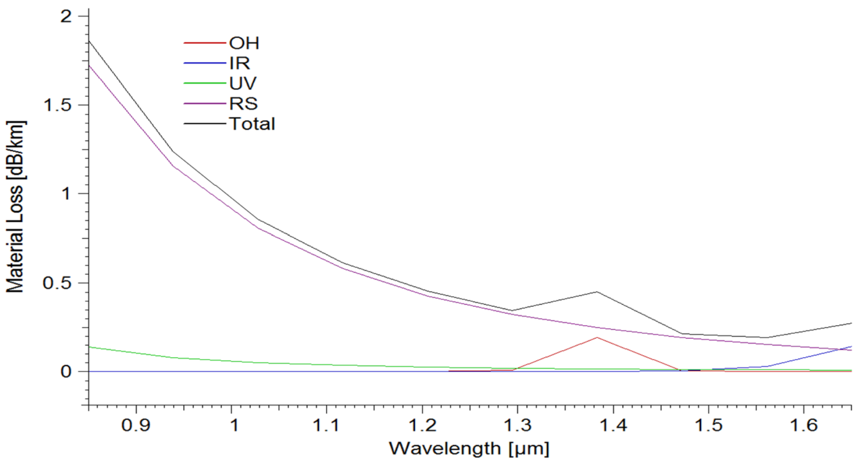

Figure 6: Total fibre material losses variations with the fibre wavelength variations.

increases linearly with wavelength. Mode field diameter increases linearly from the value of 15.4–17.2 μm with fibre wavelength variations. Besides the effective fibre area increases linearly with the fibre wavelength variations. The effective fibre area is 230 μm^2 at 1.65 μm and the effective fibre area is 180 μm^2 at 0.85 μm.

Figure 6 shows the total fibre material losses variations with the fibre wavelength variations. The OH fibre peak loss is 0.25 dB/km at 1.39 μm. The infrared (IR) fibre loss has 0.3 dB/km at 1.65 μm. The ultraviolet (UV) fibre loss decreases linearly to reach 0.01 dB/km at 1.65 μm, while the value of 0.2 dB/km at 0.85 μm. The Rayleigh scattering (RS)

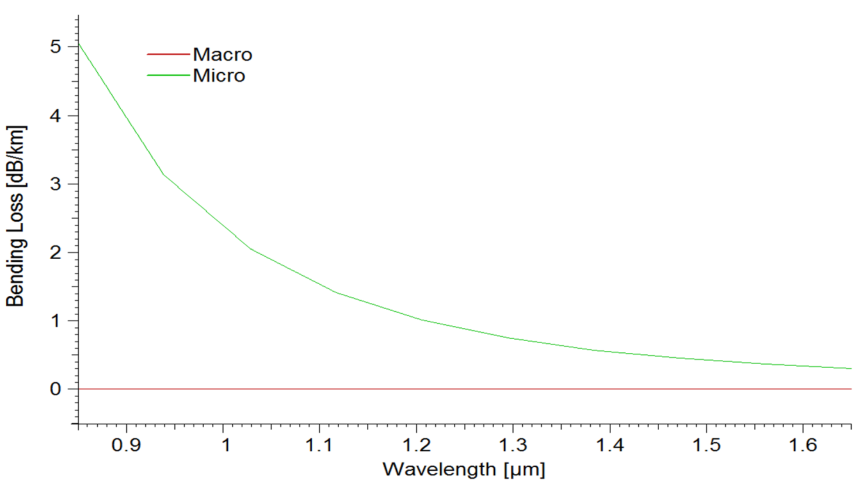

Figure 7: Macro/micro fibre bending losses variations versus the fibre wavelength variations.

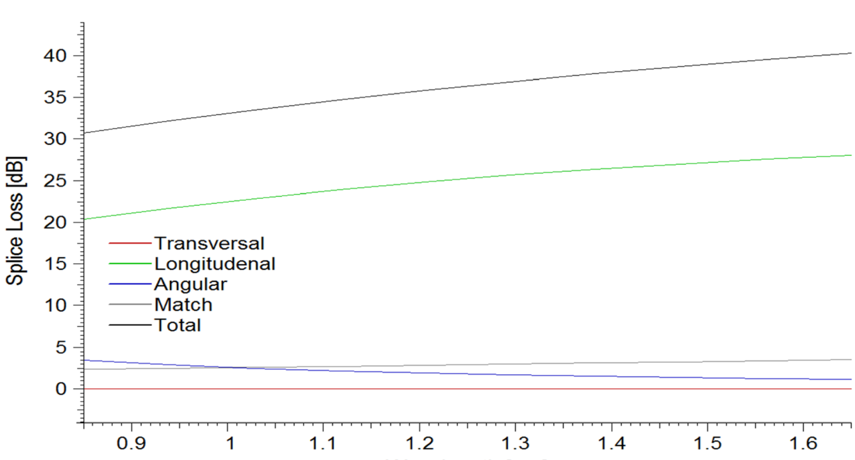

Figure 8: Total fibre splice loss variations against the fibre wavelength variations.

fibre loss decreases exponentially with fibre wavelength variations. Where the max RS fibre loss value is 1.7 dB/km at 0.85 µm, but the min RS fibre loss value is 0.325 dB/km at 1.65 µm. Therefore the resultant total fibre material loss decreases linearly with fibre wavelength variations. Where the total fibre material loss value is 1.852 dB/km at 0.85 µm, but the min total fibre material loss value is 0.3786 dB/km at 1.65 µm.

Figure 7 shows the micro/macro fibre losses of the bending variations versus the fibre wavelength variations. The micro fibre bending loss decreases exponentially from 5 to 0.5 dB/km with the fibre wavelength variations. But the macro fibre bending loss is approximately zero.

Figure 8 demonstrates the total fibre splice loss variations against the fibre wavelength variations. The transversal splice loss is approximately zero, the longitudinal

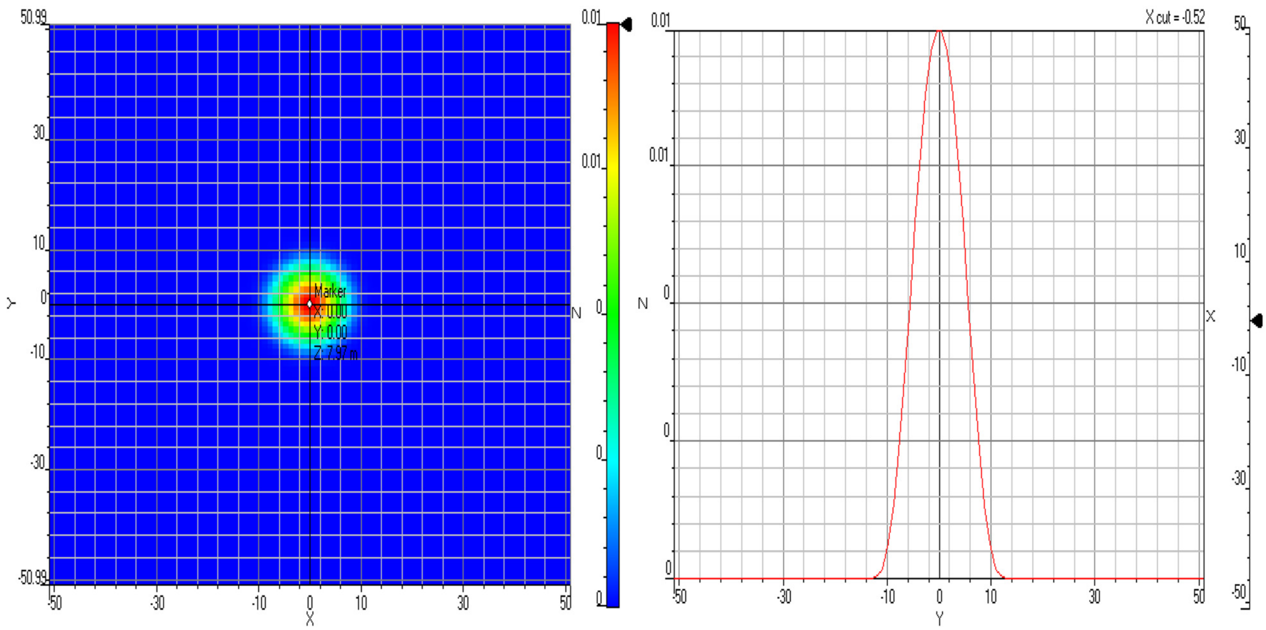

Figure 9: Dominant mode field (DMF) distribution for LP (0, 1) 1.4493825.

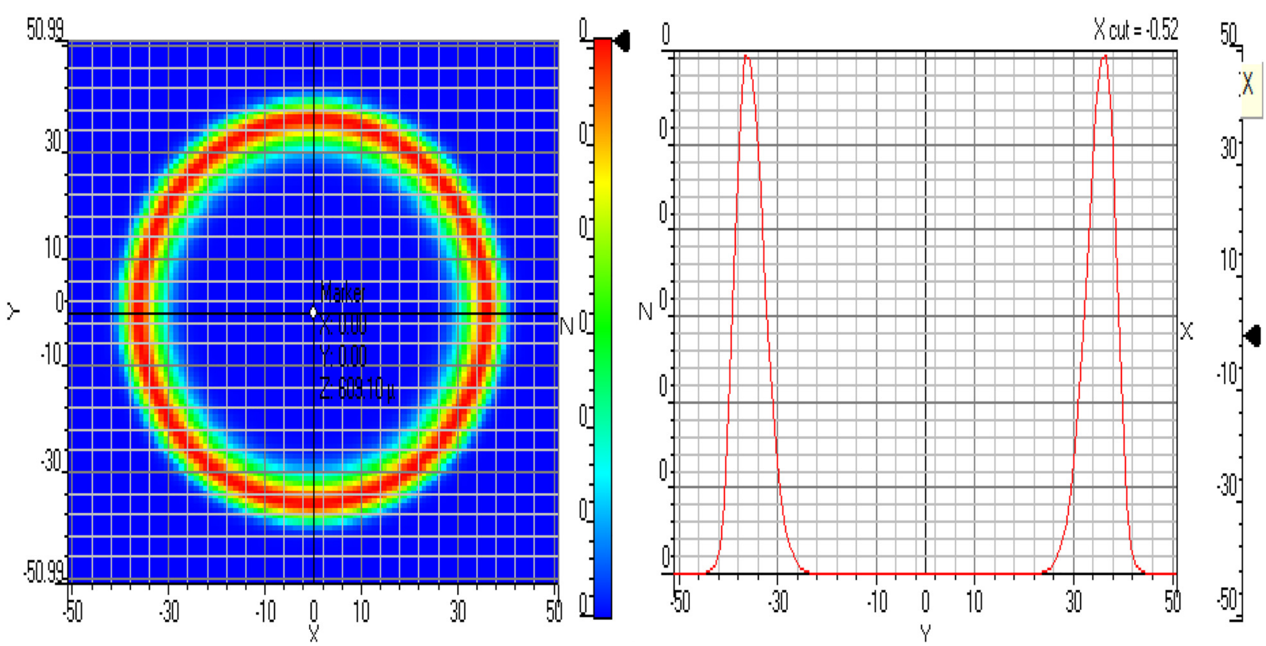

Figure 10: DMF distribution for LP (0, 2) 1.4485248.

splice loss increases slightly in linear relation from 20 to 25 dB with the fibre wavelength variations from 0.85 to 1.65 μm. Where the angular splice loss decreases linearly from 3 to 0.5 dB. But the match splice loss increases linearly from 2.5 to 5 dB with the fibre wavelength variations. The total fibre splice loss increases linearly from 30 to 40 dB.

The set of Figures 9–13 clarify the dominant mode field distribution for LP (0, 1)-> 1.4493825, LP (0, 2) -> 1.4485248, LP (0, 3) -> 1.4469608, LP (0, 4) -> 1.4468666 and LP (0, 5) -> 1.4455431. The mode field distribution is assured in all figures in *x*, *y*, *z* directions respectively. Where the other modes for designed multi-layer fibre are LP (1, 1) -> 1.4485126, LP (1, 2) -> 1.4484474, LP (1, 3) -> 1.4469447, LP (1, 4) -> 1.4455295, LP (1, 5) -> 1.4452064. While the fibre ITU-T values for the different modes based the designed multi-layer fibre is LP (1, 1) -> 5.9500000.

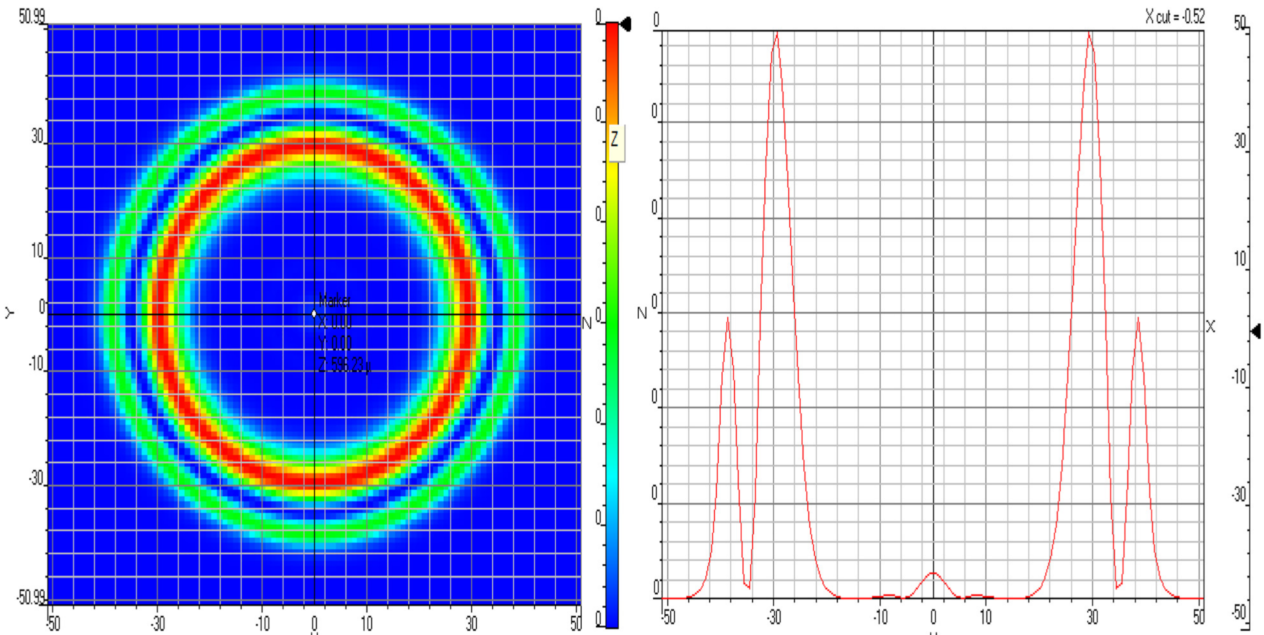

Figure 11: DMF distribution for LP (0, 3) 1.4469608.

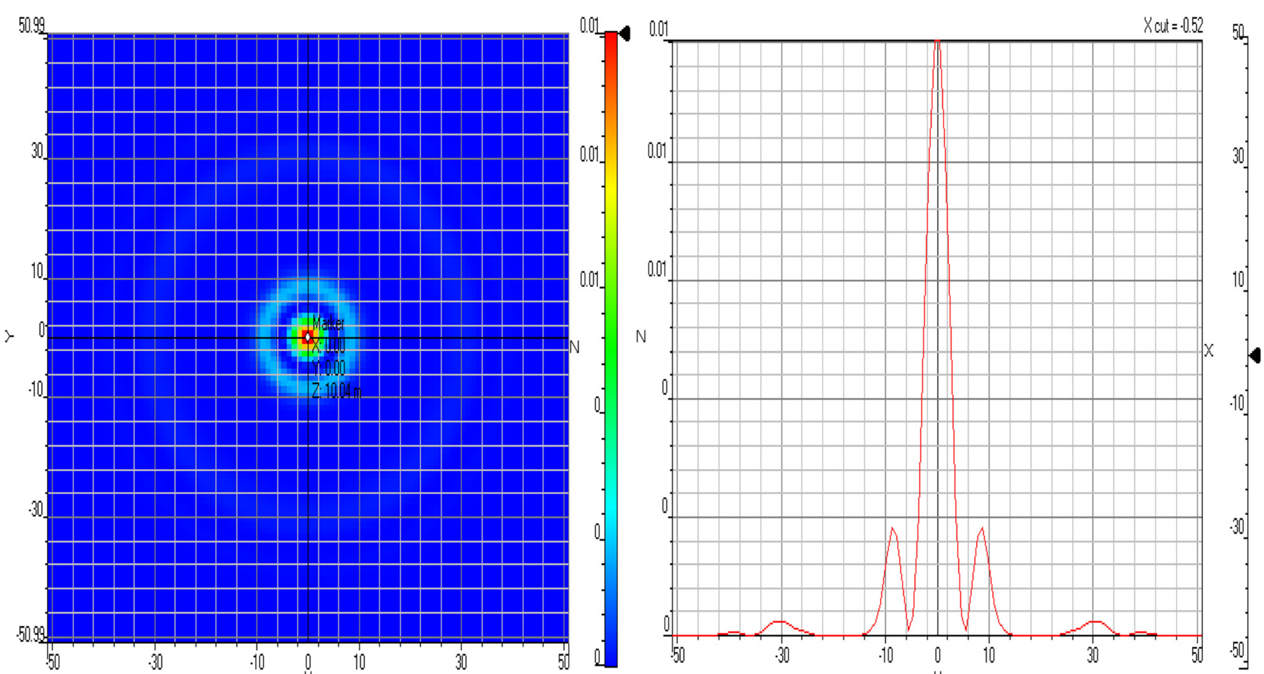

Figure 12: DMF distribution for LP (0, 4) 1.4468666.

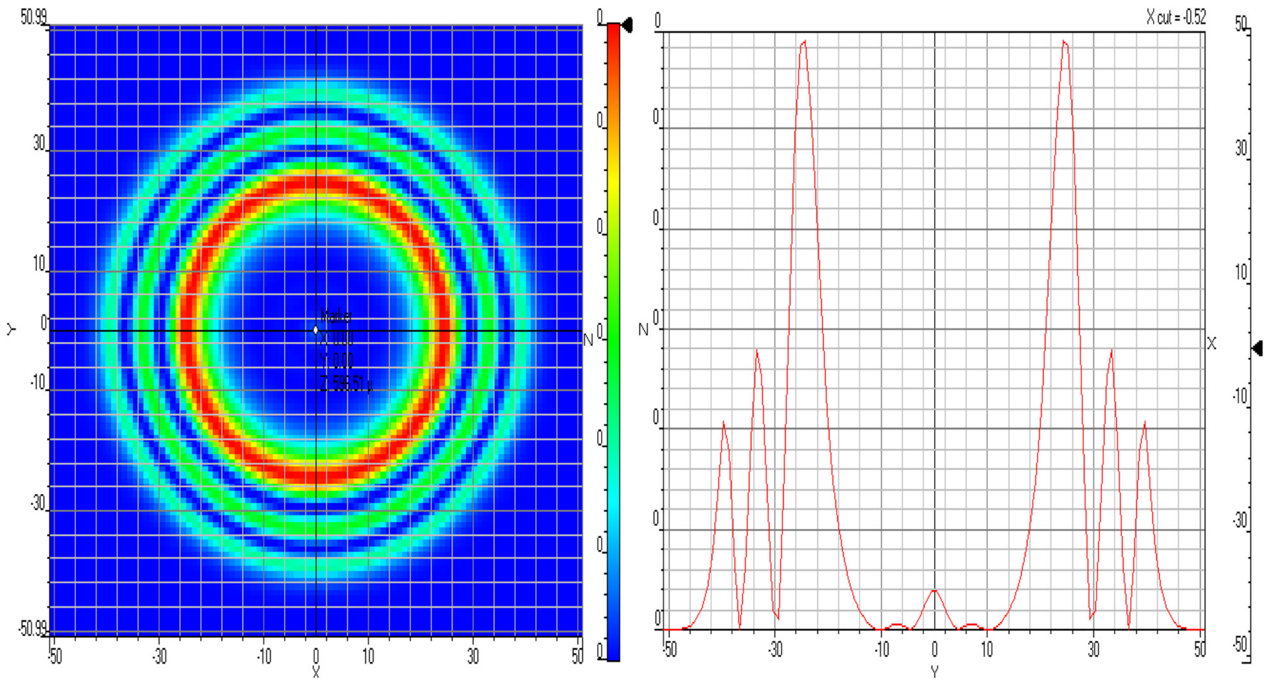

Figure 13: DMF distribution for LP (0, 5) 1.4455431.

4 Conclusions

The designed multi-layer fibre is simulated by using optifibre simulation software. The model/group RI is demonstrated with fibre wavelength variations. All the fibre losses and fibre dispersion are simulated and clarified in more details. All the fibre linear polarization (LP) modes and the theoretical fibre cutoff values for the different modes based the designed fibre profile model are detected and clarified by using the finite difference method. The study assured that the zero dispersion for the designed multi fibre layer is at 1.2689 μm and the slope of dispersion is 0.1069 ps/nm^2 km for the designed fibre. More attempts and new research work are performed to reduce the fibre propagation problems.

Author contributions: All the authors have accepted responsibility for the entire content of this submitted manuscript and approved submission.

Research funding: None declared.

Conflict of interest statement: The authors declare no conflicts of interest regarding this article.

References

1. Kao CK, Boyle WS, Smith GE. Transmission of light by fibres for optical communication. Contrib Sci (Los Angel) 2011;7:109–15.
2. Lathief KA. Attenuation measurement in optical fibre communication. Int J Res Stud Sci Eng Tech (IJRSSET) 2014;1:62–7.
3. Rashed ANZ, Gawad Mohamed AE-NAE, Hanafy SAERS, Aly MH. A comparative study of the performance of graded index perfluorinated plastic and alumino silicate optical fibres in internal optical interconnections. Optik 2016;127:9259–63.
4. Rashed ANZ, Mohamed AEl-NA, Mostafa S, El-Samie FEA. Performance evaluation of SAC-OCDMA system in free space optics and optical fibre system based on different types of codes. Wirel Pers Commun J 2017;96:2843–61.
5. Rashed ANZ, Tabbour MSF. Suitable optical fibre communication channel for optical nonlinearity signal processing in high optical data rate systems. Wirel Pers Commun J 2017;97:397–416.
6. Rashed ANZ, Tabbour MSF, Meadawy SE. Optimum flat gain with optical amplification technique based on both gain flattening filters and fibre bragg grating methods. J Nanoelectron Optoelectron 2018;13:665–76.
7. Nasr Mohamed SED, Mohamed AEl-NA, El-Samie FEA, Rashed ANZ. Performance enhancement of IM/DD optical wireless systems. Photonic Netw Commun 2018;36:114–27.
8. Rashed ANZ, Tabbour MSF. The trade off between different modulation schemes for maximum long reach high data transmission capacity optical orthogonal frequency division multiplexing (OOFDM). Wirel Pers Commun J 2018;101:325–37.
9. Rashed ANZ, Kader HMA, Awamry AAA, Abd El-Aziz IA, Transmission performance simulation study evaluation for high speed radio over fibre communication systems. Wirel Pers Commun J 2018;103:1765–79.
10. Rashed ANZ, Tabbour MSF. Best candidate integrated technology for low noise, high speed, and wide bandwidth based transimpedance amplifiers in optical computing systems and optical fibre applications. Int J Commun Sys 2018;31:e3801.

11. Rashed ANZ, Tabbour MSF, Assar ME. 20 Gb/s hybrid CWDM/DWDM for extended reach fibre to the home network applications. Proc Natl Acad Sci India Sect A Phys Sci 2018;89:653–62.
12. Costa B, Mazzoni D, Puleo M, Vezzoni E. Phase shift technique for the measurement of chromatic dispersion in optical fibres using LED's. IEEE J Quant Electron 1982;18:1509–15.
13. Merritt P, Tatam RP, Jackson DA. Interferometric chromatic dispersion measurements on short lengths of monomode optical fibre. J Lightwave Technol 1989;7:703–16.
14. Praveen Chakkravarthy S, Arthi V, Karthikumar S, Rashed ANZ, Yupapin P, Amiri IS. Ultra high transmission capacity based on optical first order soliton propagation systems. Results Phys 2019;12:512–3.
15. Rashed ANZ, Vinoth Kumar K, Prithi S, Maheswar R, Tabbour MSF. Transmittivity/reflectivity, bandwidth, and ripple factor level measurement for different refractive index fibre grating shape profiles. J Opt Commun 2019 Feb 6. https://doi.org/10.1515/joc-2018-0233 [Epub ahead of print].
16. Rashed ANZ, Vinoth Kumar K, Venkatesh Kumar P, Mohamed AE-NA, Tabbour MS, El-Assar M. DWDM channel spacing effects on the signal quality for DWDM/CWDM FTTx network. J Opt Commun 2019 Feb 7. https://doi.org/10.1515/joc-2019-0012 [Epub ahead of print].
17. Rashed ANZ, Tabbour MSF, Vijayakumari P. Numerical analysis of optical properties using octagonal shaped photonic crystal fibre. J Opt Commun 2019 Feb 8. https://doi.org/10.1515/joc-2019-0013 [Epub ahead of print].
18. Rashed ANZ, Satheesh Kumar S, Tabbour MSF, Sundararajan TVP, Maheswar R. Different graded refractive index fibre profiles design for the control of losses and dispersion effects. J Opt Commun 2019 Feb 19. https://doi.org/10.1515/joc-2019-0036 [Epub ahead of print].
19. Rashed ANZ. Comparison between NRZ/RZ modulation techniques for upgrading long haul optical wireless communication systems. J Opt Commun 2019 Feb 19. https://doi.org/10.1515/joc-2019-0038 [Epub ahead of print].
20. Rashed ANZ, Vinoth Kumar K, Tabbour MSF, Sundararajan TVP. Nonlinear characteristics of semiconductor optical amplifiers for optical switching control realization of logic gates. J Opt Commun 2019 Feb 19. https://doi.org/10.1515/joc-2019-0027 [Epub ahead of print].
21. Ahmed K, Kumar Paula B, Vasudevan B, Rashed ANZ, Maheswar R, Amiri IS, et al. Design of D-shaped elliptical core photonic crystal fibre for blood plasma cell sensing application. Results Phys 2019;12:2021–5.
22. Al-Bazzaz SHS. Simulation of single mode fibre optics and optical communication components using VC++. Int J Netw Secur 2008;8:300–8.
23. Grabka M, Wajnchold B, Pustelny S, Gawlik W. Experimental and theoretical study of light propagation in suspended-core optical fibre. Acoust Sci Technol 2010;118:1127.
24. Salleh MFM, Zakaria Z. Optical power attenuation of long distance OPGW in Malaysia. J Theor Appl Inf Technol 2015;75:331–5.
25. Amiri IS, Rashed ANZ, Yupapin P. Influence of device to device interconnection elements on the system behavior and stability. Indones J Electr Eng Comput Sci 2020;18:843–7.
26. Eid MMA, Amiri IS, Zaki Rashed AN, Yupapin P, Dental lasers applications in visible wavelength operational band. Indones J Electr Eng Comput Sci 2020;18:890–5.
27. Amiri IS, Rashed ANZ, Yupapin P. Comparative simulation study of multi stage hybrid all optical fibre amplifiers in optical communications. J Opt Commun 2020 Feb 4. https://doi.org/10.1515/joc-2019-0132 [Epub ahead of print].
28. Amiri IS, Rashed ANZ, Abdel Kader HM, Al-Awamry AA, Abd El-Aziz IA, Yupapin P, et al. Optical communication transmission systems improvement based on chromatic and polarization mode dispersion compensation simulation management. Optik J 2020;207:163853.
29. Samanta D, Sivaram M, Rashed ANZ, Boopathi CS. Amiri IS, Yupapin P. Distributed feedback laser (DFB) for signal power amplitude level improvement in long spectral band. J Opt Commun 2020 Apr 2. https://doi.org/10.1515/joc-2019-0252 [Epub ahead of print].
30. Amiri IS, Rashed ANZ, Yupapin P. Analytical model analysis of reflection/transmission characteristics of long-period fibre Bragg grating (LPFBG) by using coupled mode theory. J Opt Commun 2020 Apr 2. https://doi.org/10.1515/joc-2019-0187 [Epub ahead of print].
31. Amiri IS, Rashed ANZ, Rahman Z, Paul BK, Ahmed K. Conventional/phase shift dual drive Mach–Zehnder modulation measured type based radio over fibre systems. J Opt Commun 2020 Apr 14. https://doi.org/10.1515/joc-2019-0312 [Epub ahead of print].
32. Alatwi AM, Rashed ANZ, El-Eraki AM, Amiri IS. Best candidate routing algorithms integrated with minimum processing time and low blocking probability for modern parallel computing systems. Indones J Electr Eng Comput Sci 2020;19:847–54.
33. El-Hageen HM, Alatwi AM, Rashed ANZ. Silicon-germanium dioxide and aluminum indium gallium arsenide-based acoustic optic modulators. Open Eng Journal 2020;10:506–11.
34. Zendhnam A, Mirzaei M, Farashiani A, Farahani LH. Investigation of bending loss in a single-mode optical fibre. Pramana – J Phys 2010;74:591–603.
35. Salleh MFM, Zakaria Z. Effect of bending optical fibre on bend loss over a long period of time. ARPN J Eng Appl Sci 2015;10:45–65.
36. Taha SA, Shellal MM, Kadhim AC. Simulation of Gaussian pulses propagation through single mode optical fibre using MATLAB. Iraqi J Sci 2013;54:601–6.
37. Lawan SH, Ajiya M, Shuaibu DS. Numerical simulation of chromatic dispersion and fibre attenuation in a single-mode optical fibre system. IOSR-JECE 2012;3:31–4.
38. García S, Gasulla I. Universal characteristic equation for multi-layer optical fibres. IEEE J Sel Top Quant Electron 2020;26:4300111.
39. Oglah MH. Estimate the attenuation and simulation of dispersion Gaussian pulses propagation in a single mode optical fibre. Tikrit J Pure Sci 2017;22:108–14.
40. Ahmed K, AlZain MA, Abdullah H, Luo Y, Vigneswaran D, Faragallah OS, et al. Highly sensitive twin resonance coupling refractive index sensor based on gold- and MgF_2-coated nano metal films. Biosensors 2021;11:104.
41. Samira Delwar T, Siddique A, Ranjan Biswal M, Rashed ANZ, Jana Jee A, Ryu Y. Novel multi-user MC-CSK modulation technique in visible light communication. Opt Quant Electron 2021 Apr 3. https://doi.org/10.1007/s11082-021-02784-4 [Epub ahead of print].
42. Eid MMA, Ahasan Habib M, Shamim Anower M, Rashed ANZ. Hollow core photonic crystal fibre (PCF)–based optical sensor for

blood component detection in terahertz spectrum. Braz J Phys 2021 Apr 17. https://doi.org/10.1007/s13538-021-00906-7 [Epub ahead of print].
43. Eid MMA, Sorathiya V, Lavadiya S, El-Hamid HSA, Rashed ANZ. Wide band fibre systems and long transmission applications based on optimum optical fibre amplifiers lengths. J Opt Commun 2021 Apr 20. https://doi.org/10.1515/joc-2021-0020 [Epub ahead of print].
44. Eid MMA, Sorathiya V, Lavadiya S, El-Hamid HSA, Rashed ANZ. Optical switches based semiconductor optical amplifiers (SOAs) for performance characteristics enhancement by using various electrical pulse generators. J Opt Commun 2021 May 3. https://doi.org/10.1515/joc-2021-0066 [Epub ahead of print].
45. Eid MMA, Rashed ANZ, Sorathiya V, Lavadiya S, Ahasan Habib M, Sadegh Amiri I. GaAs electro-optic absorption modulators performance evaluation, under high-temperature variations. J Opt Commun 2021 May 3. https://doi.org/10.1515/joc-2020-0011 [Epub ahead of print].
46. Abdullaha H, Ahmed K, Alama MS, Rashed ANZ, Mitua SA, Al-Zahranid FA, et al. High sensitivity refractive index sensor based on triple layer MgF_2-gold-MgF_2 coated nano metal films photonic crystal fibre. Optik (Stuttg) 2021;241:166950.
47. Eid MMA, Sorathiya V, Lavadiya S, Abd El-Aziz IA, Rashed ANZ. Free space optics communication channel with amplitude/frequency shift keying modulation technique based raised cosine line coding. J Opt Commun 2021 May 13. https://doi.org/10.1515/joc-2021-0037 [Epub ahead of print].
48. Eid MMA, Rashed ANZ, Rajagopal M, Parimanam J, Abhay V. Integrated role between VCSEL diodes and Gaussian pulse generators with ideal EDFA for self phase modulation instability management. J Opt Commun 2021 May 20. https://doi.org/10.1515/joc-2020-0251 [Epub ahead of print].
49. Jeon KS, Kim HJ, Kang DS, Pan JK. Optical fibre chromatic dispersion measurement using bidirectional modulation of an optical intensity modulator. IEEE Photon Technol Lett 2002;14:1145–7.
50. Taga H, Yamamoto S, Edagawa N, Yoshida Y, Akiba S, Wakabayashi H. Fibre chromatic dispersion equalization at the receiving terminal of IM-DD ultra-long distance optical communication systems. J Lightwave Technol 1994;12:1042–6.
51. Ma T, Markov A, Wang L, Skorobogatiy M. Graded index porous optical fibres dispersion management in terahertz range. Opt Express 2015;23:7856–69.
52. Al-Mamun Bulbul A, Rashed ANZ, El-Hageen HM, Alatwi AM. Design and numerical analysis of an extremely sensitive PCF-based sensor for detecting kerosene adulteration in petrol and diesel. Alex Eng J 2021;60:5419–30.
53. Eid MMA, Sorathiya V, Lavadiya S, Abd El-Aziz IA, Asaduzzaman S, Rehana H, et al. ROF systems performance efficiency based on continuous phase frequency shift keying phase modulation scheme. J Opt Commun 2021 Jun 7. https://doi.org/10.1515/joc-2021-0061 [Epub ahead of print].
54. Ahasan Habib M, Shamim Anower M, Ahmed AG, Faragallah OS, Eid MMA, Rashed ANZ. Efficient way for detection of alcohols using hollow core photonic crystal fibre sensor. Opt Rev 2021 Jun 22. https://doi.org/10.1007/s10043-021-00672-6 [Epub ahead of print].
55. Eid MMA, Sorathiya V, Lavadiya S, Parmar J, Patel SK, Ahmed Ali S, et al. CWDM communication system based inline erbium-doped fibre amplifiers with the linear geometrical polarization model. J Opt Commun 2021 Jul 10. https://doi.org/10.1515/joc-2021-0033 [Epub ahead of print].
56. Sorathiya V, Lavadiya S, Ahmed AG, Faragallah OS, El-sayed HS, Mahmoud M, et al. A comparative study of broadband solar absorbers with different gold metasurfaces and MgF_2 on tungsten substrates. J Comput Electron 2021 Jul 16. https://doi.org/10.1007/s10825-021-01746-z [Epub ahead of print].
57. Lavadiya SP, Sorathiya V, Kanzariya S, Chavda B, Faragallah OS, Eid MMA, et al. Design and verification of novel low profile miniaturized pattern and frequency tunable microstrip patch antenna using two PIN diodes. Braz J Phys 2021 Aug 2. https://doi.org/10.1007/s13538-021-00951-2 [Epub ahead of print].
58. Eid MMA, Urooj S, Muhammad Alwadai N, Rashed ANZ. AlGaInP optical source integrated with fibre links and silicon avalanche photo detectors in fibre optic systems. Indones J Electr Eng Comput Sci 2021;23:847–854.
59. Urooj S, Muhammad Alwadai N, Ibrahim A, Rashed ANZ. Simulative study of raised cosine impulse function with hamming grating profile based chirp Bragg grating fibre. J Opt Commun 2021 Aug 6. https://doi.org/10.1515/joc-2021-0062 [Epub ahead of print].
60. Jibon RH, Bulbul AAM, Rashed ANZ, Faragallah OS, Baz M, Mahmoud M, et al. Design and numerical analysis of a photonic crystal fibre (PCF)-based flattened dispersion THz waveguide. Opt Rev 2021 Aug 25. https://doi.org/10.1007/s10043-021-00698-w [Epub ahead of print].
61. Eid MMA, Mohammed AE-NA, Rashed ANZ. Different soliton pulse order effects on the fibre communication systems performance evaluation. Indones J Electr Eng Comput Sci 2021;23:1485–92.
62. Urooj S, Muhammad Alwadai N, Sorathiya V, Lavadiya S, Parmar J, Patel SK, et al. Differential coding scheme based FSO channel for optical coherent DP-16 QAM transceiver systems. J Opt Commun 2021 Sep 27. https://doi.org/10.1515/joc-2021-0118 [Epub ahead of print].
63. Fiol G, Lott JA, Ledentsov NN, Bimberg D. Multimode optical fibre communication at 25 Gbit/s over 300 m with small spectral-width 850 nm VCSELS. Electron Lett 2011;47:810–1.
64. Downie JD, Hurley JE, Kuksenkov DV, Lynn CM, Korolev AE, Nazarov VN. Transmission of 112 Gb/s PM-QPSK signals over up to 635 km of multimode optical fibre. Opt Express 2011;19:B363–9.
65. Rashed ANZ, Fawzy Zaky W, El-Hageen HM, Alatwi AM. Technical specifications for an all-optical switch for information storage and processing systems. Eur Phys J Plus 2021;136:1100.
66. Sorathiya V, Lavadiya S, Parmar B, Das S, Krishna M, Faragallah OS, et al. Numerical investigation of the tunable polarizer using gold array and graphene metamaterial structure for an infrared frequency range. Appl Phys B 2022;128:13.
67. Delwar TS, Siddique A, Biswal MR, Behera P, Rashed ANZ, Choi Y, et al. A novel dual mode configurable and tunable high-gain, high-efficient CMOS power amplifier for 5G applications. Integrat VLSI J 2022;83:77–87.
68. Eid MMA, Arunachalam R, Sorathiya V, Lavadiya S, Patel SK. Parmar J, et al. QAM receiver based on light amplifiers measured

with effective role of optical coherent duobinary transmitter. J Opt Commun 2022 Jan 17. https://doi.org/10.1515/joc-2021-0205 [Epub ahead of print].
69. Sorathiya V, Lavadiya S, Ahmed AG, Faragallah OS, El-Sayed HS, Parmar B, et al. Hilbert resonator based multiband tunable graphene metasurface polarizer for lower THz frequency. J Comput Electron 2022 Jan 22. https://doi.org/10.1007/s10825-021-01848-8.
70. Mohammad A, Alzaidi MS, Mahmoud M, Eid A, Sorathiya V, Lavadiya S, et al. First order surface grating fibre coupler under the period chirp and apodization functions variations effects. Indones J Electr Eng Comput Sci 2022;25:1020–9.
71. Mohammad A, Alzaidi MS, Mahmoud M, Eid A, Sorathiya V, Lavadiya S, et al. Free space optical communication system for indoor applications based on printed circuit board design. Indones J Electr Eng Comput Sci 2022;25:1030–7.
72. Sorathiya V, Lavadiya S, Singh Parmar B, Baxi S, Dhankot T, Faragallah OS, et al. Tunable squared patch based graphene metasurface infrared polarizer. Appl Phys B 2022 Jan 30. https://doi.org/10.1007/s00340-022-07765-3 [Epub ahead of print].
73. Lavadiya S, Sorathiya V, Faragallah OS, El-Sayed HS, Mahmoud M, Eid A, et al. Infrared graphene assisted multi-band tunable absorber. Opt Quant Electron 2022;54:134.
74. Habib Jibon R, Ahmed M, Abd-Elnaby M, Rashed ANZ, Mahmoud M, Eid A. Design mechanism and performance evaluation of photonic crystal fibre (PCF) based sensor in the THz regime for sensing noxious chemical substrates of poultry feed. Appl Phys A 2022;128:169.
75. Sorathiya V, Lavadiya S, Thomas L, Abd-Elnaby M, Rashed ANZ, Mahmoud M, et al. Graphene based tunable short band absorber for infrared wavelength. Appl Phys B 2022;128:40.
76. Dutta N, Patel SK, Faragallah OS, Baz M, Rashed ANZ. Caching scheme for information-centric networks with balanced content distribution. Int J Commun Syst 2022:e5104. https://doi.org/10.1002/dac.5104.
77. Miller SE, Kaminow IP, editors. Optical fibre telecommunications II. Boston: Academic Press; 1988.
78. Poole CD, Winters JH, Nagel JA. Dynamical equation for polarization dispersion. Opt Lett 1991;16:372–4.
79. Al-Khaffaf DAJ, Rashid Hujijo HS. High data rate optical wireless communication system using millimeter wave and optical phase modulation. ARPN J Eng Appl Sci 2018;13:9086–92.
80. Al-Khaffaf DAJ, Alshimaysawe IA. Miniaturised tri-band microstrip patch antenna design for radio and millimetre waves of 5G devices. Indones J Electr Eng Comput Sci 2021;21:1594–601.
81. Al-Khaffaf DAJ, Alsahlany AM. A cloud VLC access point design for 5G and beyond. Opt Quant Electron 2021;53:472–81.
82. Al-Khaffaf DAJ, Alsahlany AM. 60 GHz millimetre wave/10 gbps transmission for super broadband Wi-fi network. J Commun 2019;14:261–6.
83. Aly MH. Performance evaluation of 6.4 Tbps dual polarization quadrature phase shift keying Nyquist-WDM superchannel FSO transmission link: impact of weather conditions. Alex Eng J 2020;59:977–86.
84. Singh M, Malhotra J. A high-speed long-haul wavelength division multiplexing-based inter-satellite optical wireless communication link using spectral-efficient 2-D orthogonal modulation scheme. Int J Commun Syst 2020;33:e4293.
85. Marcuse D. Principle of optical fibre measurements. New York: Academic Press; 1981.
86. Rashed ANZ. High reliability optical interconnections for short range applications in high speed optical communication systems. Opt Laser Technol 2013;48:302–8.
87. Rashed ANZ. High performance photonic devices for multiplexing/demultiplexing applications in multi band operating regions. J Comput Theor Nanosci 2012;9:522–31.
88. Rashed ANZ. Optical fibre communication cables systems performance under harmful gamma irradiation and thermal environment effects. IET Commun 2013;7:448–55.
89. Rashed ANZ. Submarine fibre cable network systems cost planning considerations with achieved high transmission capacity and signal quality enhancement. Opt Commun 2014;311:44–54.
90. Hossain E, Hossain MS, Hossain MS, Jannat SA, Huda M, Alsharif S, et al. Brain tumor auto-segmentation on multimodal imaging modalities using deep neural network. Comput Mater Continua (CMC) 2022;72:4509–23.
91. Asaduzzaman S, Rehana H, Rana C, Faragallah OS, El-Sayed HS, Mahmoud M, et al. Hexa sectored square photonic crystal fibre for blood serum and plasma sensing with ultralow confinement loss. Appl Phys A 2022;128:467.
92. Omollo Nyangaresi V, Abd-Elnaby M, Mahmoud M, Eid A, Rashed ANZ. Trusted authority based session key agreement and authentication algorithm for smart grid networks. Trans Emerging Tel Tech Journal 2022;35:1–16.
93. Sunitha G, Arunachalam R, Abd-Elnaby M, Mahmoud M, Eid A, Rashed ANZ. A comparative analysis of deep neural network on acoustic cough features. Int J Imag Syst Technol 2022;52:1–14.
94. Lavadiya SP, Sorathiya V, Kanzariya S, Chavda B, Naweed A, Faragallah OS, et al. Low profile multiband microstrip patch antenna with frequency reconfigurable feature using PIN diode for S, C, X, and Ku band applications. Int J Commun Syst 2022;35:e5141.
95. Asaduzzaman S, Rehana H, Aziz T, Faragallah OS, Baz M, Mahmoud M, et al. Key performance parameters estimation with Epsilon near zero (ENZ) for Kagome photonic crystal fibre in THz system. Opt Quant Electron 2022;54:202.
96. Sorathiya V, Faragallah OS, El-Sayed HS, Mahmoud M, Eid A, Rashed ANZ. Nanofocusing of optical wave using staircase tapered plasmonic waveguide. Appl Phys B 2022;128:104.
97. Patel SK, Solanki N, Charola S, Parmar J, Zakaria R, Faragallah OS, et al. Graphene based highly sensitive refractive index sensor using double split ring resonator metasurface. Opt Quant Electron 2022;54:203.
98. Sorathiya V, Lavadiya S, Faragallah OS, Mahmoud M, Eid A, Rashed ANZ. D shaped dual core photonics crystal based refractive index sensor using graphene–titanium–silver materials for infrared frequency spectrum. Opt Quant Electron 2022;54:290.